ELSEVIER

Atmospheric Environment 38 (2004) 345–355

ATMOSPHERIC ENVIRONMENT

www.elsevier.com/locate/atmosenv

Dynamic transport of livestock generated VOC-odor in a ventilated airspace with mixing heterogeneity

Huang-Min Liang, Chung-Min Liao*

Department of Bioenvironmental Systems Engineering, National Taiwan University, Taipei, Taiwan 10617, ROC

Received 16 June 2003; received in revised form 3 October 2003; accepted 3 October 2003

Abstract

This research proposes a multiple airflow regions gamma model to simulate airflow pattern in a ventilated airspace with mixing heterogeneity based on residence time distribution and gamma distribution statistics. We select *p*-cresol, toluene and *p*-xylene, three intensive odor causing volatile organic compounds (VOC-odor) found in swine housing, to account different mixing behaviors. By fitting the VOC-odor concentration profile calculated from VOC-odor transport model with three-parameter gamma distribution, we can characterize the extent of mixing and predict mixing heterogeneity in a ventilated livestock housing. A typical swine housing with a mechanical ventilation system in southern Taiwan was selected for model simulation. Results demonstrate that the mean residence time of *p*-cresol, toluene and *p*-xylene are 44.45 ± 0.91, 267.30 ± 58.90 and 332.38 ± 129.83 h, whereas mean mixing factor are 0.20 ± 0.05, 0.81 ± 0.17, and 0.81 ± 0.19, respectively, corresponding to a ventilation rate of $0.075 \pm 0.025\ m^3\ s^{-1}\ pig^{-1}$ within manure moisture content of $70 \pm 10\%$. This research gives additional physical information to characterize mixing behavior temporally and spatially with mean residence time and mixing factor, respectively, in a ventilated airspace with mixing heterogeneity. The robustness of multiple airflow regions gamma model can offer designers to reconsider the efficiency of ventilation systems through different mixing flow patterns in place of complete mixing hypothesis.

Keywords: Mixing heterogeneity; Mixing factor; Odor; Residence time distribution; Volatile organic compounds

1. Introduction

Manure storage is a major source of odor causing volatile organic compounds and is referred to as VOC-odor (Clanton et al., 2001), which is composed from miscellaneous chemicals (Schiffman et al., 2001). Workers in swine production facilities experience dust-borne VOC-odor toxic syndrome. In addition, excessive exposure to VOC-odor can lower productivity and cause materials and equipment damage (Donham, 2000). Emission of odor from swine housing is becoming of increasing regulatory concern in Taiwan. Chung et al. (1996) made efforts on reduction ammonia and hydrogen sulfide production from pig feces by controlling environmental conditions. Chang et al. (2001) conducted an exposure assessment to airborne endotoxin, dust, ammonia, hydrogen sulfide and carbon dioxide in open style swine houses, and pointed out that employees working in the finishing stalls were exposed to the highest airborne levels of respirable endotoxin and dust. Liao et al. (2001) developed a dynamic, size-dependent integrated inhalation dose model for assessing dust-borne VOC-odor exposure from feeding in swine buildings. Great attention regarding swine VOC-odor management shows the importance of preservation of air quality and pollution source control in Taiwan.

VOC-odor generation and diffusion may be significantly influenced by the ventilation system and building configurations, which create different flow patterns (Cheng et al., 2002). Given a control volume with a defined inlet and outlet, two kinds of ideal flow patterns are theoretically possible (Levenspiel, 1999). Both piston

*Corresponding author. Tel.: +886-2-2363-4512; fax: +886-2-2362-6433.

E-mail address: cmliao@ccms.ntu.edu.tw (C.-M. Liao).

1352-2310/$ - see front matter © 2003 Elsevier Ltd. All rights reserved.
doi:10.1016/j.atmosenv.2003.10.023

flow and complete mixing flow regimes represent the limiting cases that seldom occur in a heterogeneously ventilated airspace. Young et al. (2000) suggested that incomplete mixing does occur, particularly under winter ventilation conditions, which sufficient frequency to warrant consideration in the design procedure.

Several approaches have been suggested for predicting indoor concentrations when mixing is incomplete, including ventilation efficiency and age-of-air concepts (Karimipanah and Awbi, 2002), the application of computational fluid dynamics (Huang and Haghighat, 2002), and multizone models (Wong et al., 2003). This study proposes a multiple airflow regions gamma model (MARGM) to find out residence time distribution (RTD) and mixing characteristics of VOC-odor in a heterogeneously ventilated airspace. Determining time-dependent VOC-odor concentration resulting from an instantaneous source, we consider two main physical processes of (1) transport phenomenon of the source and (2) general concentration decay due to ventilation. By fitting concentration versus time profile with three-parameter gamma distribution, we can estimate the RTD and mixing factor of different VOC-odor in swine buildings.

2. Materials and methods

2.1. VOC-odor transport model

A typical pig housing situated in Tainan, southern Taiwan region, which consists of twelve compartments with partially slatted floor, is chosen for the study purpose (Fig. 1). This pig housing has one negative pressure ventilation system of three high endwall exhaust fans with the opposite side endwall with continuous inlet fans. Each compartment contained six pigs. The body weight of each growing pig was estimated to be 70 kg. The environmental parameters used under a normal temperature and pressure conditions with a pH ranged between 8 and 9 of pig slurry are given in Table 1 (Liang, 2002).

Because *p*-cresol, which presenting a product from toluene oxidation, was one of the most intense and unpleasant VOC-odor appeared in swine housing (Louhelainen et al., 2001). We selected *p*-cresol, toluene and *p*-xylene as the study compounds. The chemical database contained pertinent physiochemical properties of study compounds, such as Henry's constant (K_H), organic carbon distribution coefficient (K_{oc}), air and water diffusion coefficients (D_g^a and D_l^w), and first-order degradation rate constant (μ), are shown in Table 2.

The VOC-odor transport model presented in this paper was adopted from Jury et al. (1990) and based on the following assumptions to simplify the specific physicochemical and biological aspects: (1) the contaminated source was uniformly distributed in the contaminated layer, (2) VOC-odor in the contaminated zone diffused up through a clean layer and a stagnant air boundary layer, (3) VOC-odor may reside in three phases in the clean layer zone, including adsorbed, dissolved and gaseous phases, (4) the adsorbed and dissolved phases undergone reversible and linear

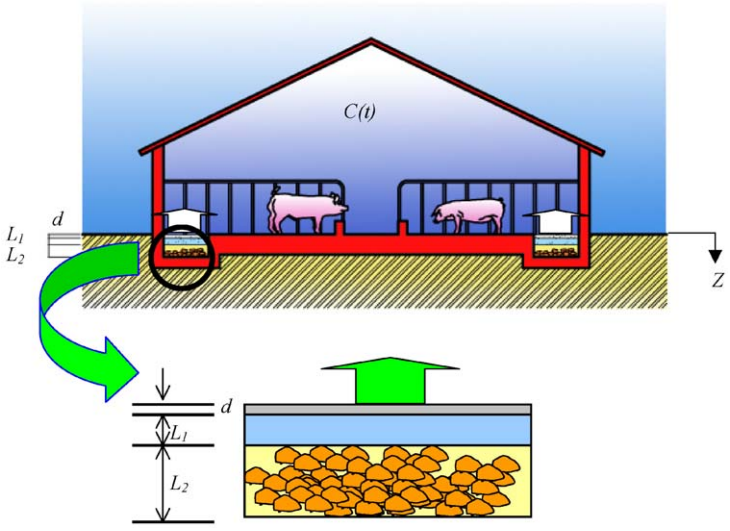

Fig. 1. The schematic of the manure-to-ventilation air pathway of VOC-odor in a pig unit with partially slatted floor. VOC-odor diffused up from the contaminated layer (L_2) through a clean layer (L_1) and a stagnant air boundary layer (d), and entered into ventilated airspace.

equilibrium adsorption, whereas dissolved and gaseous phases were in accordance with Henry's law, (5) the swine manure properties such as total porosity, gas filled porosity, bulk density, fraction of organic carbon, pH, and temperature were constant in space and time, (6) the VOC-odor moved in one dimension through swine manure and followed the principle of mass balance, (7) VOC-odor entered into a ventilated airspace by advection and diffusion, and (8) swine manure was isotropic and homogeneous.

In analogy to the behavior assessment model of Jury et al. (1990), the VOC-odor flux at the stored swine manure surface, $J_s^{net}(0,t)$, can be expressed as follows (Fig. 1),

$$J_s^{net}(0,t) = J_s(0,t;L_1+L_2) - J_s(0,t;L_1), \quad (1)$$

Table 1
Standard value of manure parameters used for model implementation in Tainan swine housing[a]

Property	Symbol	Value	Units
Porosity	ε	90	%
Moisture content	θ	70 ± 10	%
Air content[b]	ε_a	20 ± 10	%
Bulk density	ρ_b	990	$kg\,m^{-3}$
Organic carbon content	f_{oc}	0.8	%
Clean layer thickness	L_1	2	cm
Contaminated layer thickness	L_2	8	cm
Air boundary thickness	d	0.1	cm
Moisture flux rate	v_w	1.16×10^{-7}	$m\,s^{-1}$
Flux surface area	A	46	m^2
Ventilation rate	Q	0.075 ± 0.025	m^3s^{-1} per 70 kg pig
Initial concentration	C_0	1	$\mu g\,m^{-3}$

[a] Values are adopted and estimated from Liang (2002).
[b] $\varepsilon_a = \varepsilon - \theta$ (Jury et al., 1990).

where

$$J_s(0,t;L) = \frac{1}{2}C_0\exp(-\mu t)\left\{V_E\left[\mathrm{erfc}\left(\frac{vt}{\sqrt{4D_Et}}\right) - \mathrm{erfc}\left(\frac{L+vt}{\sqrt{4D_Et}}\right)\right] + (2H_E+v)\times\exp[H_E(H_E+v)t/D_E]\left[\exp(H_EL/D_E)\times\mathrm{erfc}\left(\frac{L+(2H_E+v)t}{\sqrt{4D_Et}}\right) - \mathrm{erfc}\left(\frac{(2H_E+v)t}{\sqrt{4D_Et}}\right)\right]\right\}, \quad (2)$$

in which D_E is effective diffusion coefficient ($m^2\,s^{-1}$), v is effective velocity ($m\,s^{-1}$), and H_E is boundary transfer coefficient ($m\,s^{-1}$) and can be expressed as

$$D_E = \frac{(\varepsilon_a^{10/3}D_g^aK_H + \theta^{10/3}D_l^w)/\varepsilon^2}{(\rho_bf_{oc}K_{oc} + \theta + \varepsilon_aK_H)}, \quad (3)$$

$$v = \frac{v_w}{\rho_bf_{oc}K_{oc} + \theta + \varepsilon_aK_H}, \quad (4)$$

$$H_E = \frac{K_HD_g^a}{d(\rho_bf_{oc}K_{oc} + \theta + \varepsilon_aK_H)}, \quad (5)$$

where v_w is the water velocity in manure ($m\,s^{-1}$) and d is the air boundary thickness (m). The indoor VOC-odor concentration, $C(t)$, is obtained as

$$C(t) = \frac{A}{Q}J_s^{net}(0,t) \quad (6)$$

where A is the manure surface area (m^2) and Q is the volumetric ventilation rate ($m^3\,s^{-1}$). The numerical scheme used to implement the simulations of the VOC-odor transport model was done in double precision with Visual FORTRAN on PC.

2.2. Multiple airflow regions gamma model

Our approach use gamma distribution to describe RTD function in a heterogeneously mixing ventilated airspace. The presented solution demonstrates that it is

Table 2
Physicochemical properties of study compounds

Chemical	K_{oc} (m^3kg^{-1})[a]	D_g^a ($m^2\,s^{-1}$)[a]	D_l^w ($m^2\,s^{-1}$)[b]	K_H (dimensionless)[c]	$t_{1/2}$ (d)[d]	μ (d^{-1})[e]
p-cresol	0.047	7.7×10^{-6}	7.7×10^{-10}	6.38×10^{-5}	0.67	1.034
toluene	0.126	8.8×10^{-6}	8.8×10^{-10}	0.271	22	3.15×10^{-2}
p-xylene	0.126	7.1×10^{-6}	7.1×10^{-10}	0.201	28	2.48×10^{-2}

[a] Adapted from Thibodeaux (1996).
[b] $D_l^w = D_g^a\times10^{-4}$ (Jury et al., 1990).
[c] Adapted from Weber and DiGiano (1995), where conversion factor of K_H from ($atm\,m^3\,mol^{-1}$) to dimensionless is 41.11.
[d] Adapted from Howard et al. (1991).
[e] $\mu = 0.693/t_{1/2}$.

possible to construct a systematic way of lumping parameters. In addition, the incomplete mixing behavior, such as incomplete-piston, complete-incomplete mixing flow pattern etc., could be analyzed.

The three-parameter gamma probability density function of t may be written as

$$f(t;\alpha,\beta,\gamma)=\frac{1}{\Gamma(\alpha)\cdot\beta^{\alpha}}(t-\gamma)^{\alpha-1}\exp\left(-\frac{t-\gamma}{\beta}\right),\quad \alpha>0,\beta>0,t>\gamma, \tag{7}$$

where α is the shape parameter, β is the scale parameter, and γ is the location parameter. The normalization factor $\Gamma(\alpha)=\int_0^{\infty}x^{\alpha-1}e^{-x}\,dx,\alpha>0$, where x is a dummy variable of integration, is the gamma function of mathematical statistics. In the gamma probability density function, the mean and standard deviation (sd) are mean $=\alpha\beta+\gamma$ and $sd=\alpha^{1/2}\beta$, respectively. For $\alpha=1$, Eq. (7) reduces to

$$f(t;1,\beta,\gamma)=\frac{1}{\beta}\exp\left(-\frac{t-\gamma}{\beta}\right),\quad \beta>0,t>\gamma \tag{8}$$

Since $\Gamma(\alpha)=1$ for $\alpha=1$, we can compare Eq. (8) with a special case of complete-piston flow. The complete-piston airflow model simulates a perfectly mixed airspace with a region where airflow moves in piston flow. The volume of the complete mixing flow is V_c, the volume of the piston flow is V_p, and the total volume is $V=V_c+V_p$. The complete-piston flow model is mathematical equivalent to the exponential-piston flow model defining as

$$f(t;1,\beta,\gamma)=\frac{\eta}{T}\exp\left(-\frac{\eta t}{T}+\eta-1\right),\quad t>T\left(1-\frac{1}{\eta}\right) \tag{9}$$

where

$$\eta=\frac{V_c+V_p}{V_c} \tag{10}$$

$$\beta=\frac{T}{\eta} \tag{11}$$

$$\gamma=T\left(1-\frac{1}{\eta}\right) \tag{12}$$

The general model corresponds to the general case that $V=V_c+V_p+V_i$, where V_i is the volume of incomplete mixing flow. In this case, the general model is given by Eq. (7), where parameters α, β, and γ can be derived through a deliberate mathematical computation as (Liang, 2002) (the detailed derivations may upon request from the authors)

$$\alpha=\frac{V}{V_c+V_p+\zeta V_i}=\frac{1}{\frac{1}{\kappa}+\zeta-\frac{\zeta}{\kappa}} \tag{13}$$

$$\beta=\frac{T}{\left(\frac{V}{V_c+\zeta V_i}\right)}=T\left(\frac{1}{\eta\kappa}+\zeta-\frac{\zeta}{\kappa}\right) \tag{14}$$

$$\gamma=\frac{T(\eta-1)}{\eta+\eta\zeta(\kappa-1)} \tag{15}$$

where

$$\kappa=\frac{V}{V_c+V_p} \tag{16}$$

$$\eta\kappa=\frac{V}{V_c} \tag{17}$$

in that ζ is the mixing factor describing the portion of ventilation airflow, κ and η may refer to as the mixing volume factor I and II, respectively. In order to specify its range, we can state that $\zeta=1$ for complete mixing, $\zeta=0$ for piston flow, and $0<\zeta<1$ for incomplete mixing flow. Table 3 summarized the expressions of the RTD functions of several forms of mixing patterns. These seven mixing patterns can simulate different airflow patterns by fitting the VOC-odor concentration profiles to determine the mixing heterogeneity in a ventilated airspace.

2.3. MARGM curve-fitting process

We employed @RISK (Version 4.5, Professional Edition, Palisade Corp., USA) to estimate distribution parameters. Results from goodness-of-fit statistics suggest that the gamma distribution model fits the observed data. The algorithm of using @RISK was as follows: (1) normalizing the distribution by transforming concentration versus time profile into RTD profile in such a way that the area under the curve is unity, (2) fitting the profile with three-parameter gamma distribution, and (3) giving the fitting results and distribution statistics (Fig. 2). From the minimum root mean squared error (RMSE) scenario, the best fitting parameters, including shape parameter (α), scale parameter (β), and location parameter (γ), would be determined. RMSE was calculated as follows:

$$\mathrm{RMSE}=\sqrt{\frac{\sum_{i=1}^{N}(E_{m,i}-E_{s,i})^2}{N}}, \tag{18}$$

where N denoted the number of measurements, $E_{m,i}$ (h^{-1}) was the transformed RTD value calculated from VOC-odor transport model, $E_{s,i}(h^{-1})$ was the simulation results by three-parameter gamma distribution corresponding to data point i.

From the fitting results followed by procedure illustrated in Fig. 2, we can further characterize mean resident time (T) and mean mixing factor ($\bar{\zeta}$) of different VOC-odor in swine housing. Firstly, we estimated shape parameter (α), scale parameter (β), and location parameter (γ) by curve fitting. Then, we determined mean resident time (T) by mean $=\alpha\beta+\gamma$, and calculated mixing factor ζ of incomplete mixing flow pattern and mixing volume factors of η and κ. By substituting the

Table 3
The residence time distribution (RTD) functions for different mixing patterns

Mixing pattern	RTD function
1. Complete-piston	$\frac{\eta}{T}\exp\left\{\frac{-t\eta}{T}+\eta-1\right\}, \quad t>T\left(1-\frac{1}{\eta}\right)$
2. Complete mixing	$\frac{1}{T}\exp\left\{\frac{-t}{T}\right\}, \quad t>0$
3. Piston flow	$\delta(t-T), \quad t>T$
4. Incomplete mixing	$\frac{t^{\alpha-1}}{\Gamma(\alpha)\cdot(T\zeta)^{\alpha}}\exp\left\{\frac{-t}{T\zeta}\right\}, \quad t>0$
5. Incomplete-piston	$\frac{\left\{t-\frac{T}{1+\zeta(\kappa-1)}\right\}^{\alpha-1}}{\Gamma(\alpha)\cdot\left[T\left(\frac{1}{\eta\kappa}+\zeta-\frac{\zeta}{\kappa}\right)\right]^{\alpha}}\exp\left\{\frac{-\left\{t-\frac{T}{1+\zeta(\kappa-1)}\right\}}{T\left(\frac{1}{\eta\kappa}+\zeta-\frac{\zeta}{\kappa}\right)}\right\}, \quad t>\frac{T}{1+\zeta(\kappa-1)}$
6. Complete-incomplete	$\frac{t^{\alpha-1}}{\Gamma(\alpha)\cdot\left[T\left(\frac{1}{\kappa}+\zeta-\frac{\zeta}{\kappa}\right)\right]^{\alpha}}\exp\left\{\frac{-t}{T\left(\frac{1}{\kappa}+\zeta-\frac{\zeta}{\kappa}\right)}\right\}, \quad t>0$
7. Complete-incomplete-piston	$\frac{\left\{t-\frac{T(\eta-1)}{\eta+\eta\zeta(\kappa-1)}\right\}^{\alpha-1}}{\Gamma(\alpha)\cdot\left[T\left(\frac{1}{\eta\kappa}+\zeta-\frac{\zeta}{\kappa}\right)\right]^{\alpha}}\exp\left\{\frac{-\left\{t-\frac{T(\eta-1)}{\eta+\eta\zeta(\kappa-1)}\right\}}{T\left(\frac{1}{\eta\kappa}+\zeta-\frac{\zeta}{\kappa}\right)}\right\}, \quad t>\frac{T(\eta-1)}{\eta+\eta\zeta(\kappa-1)}$

values of η and κ into Eqs. (11) and (12), the incomplete mixing volume (V_i), complete mixing volume (V_c), and piston flow volume (V_p) could be determined. Finally, we calculated mean mixing factor ($\bar{\zeta}$) of different VOC-odor by the following equation,

$$\bar{\zeta}=\frac{1\times V_c+\zeta\times V_i+0\times V_p}{V_c+V_i+V_p}. \tag{19}$$

3. Results and discussion

3.1. Predicted VOC-odor profiles

Fig. 3 presents the predicted VOC-odor profiles by transport model of Eq. (6) in that manure moisture contents (θ) varied considerably ranging from 60 to 80% depending on manure texture and environmental conditions. As θ was increased from 60 to 80%, peak air concentration of *p*-cresol increased from 3.31×10^{-14} to $6.71\times10^{-11}\,g\,m^{-3}$ and the time of peak concentration decreased from 36.5 to 34.0 h (Fig. 3a). It was resulted from effective diffusion coefficient (D_E) increased as θ increased. For toluene and *p*-xylene, D_E decreased as θ increased and resulting in peak concentration decreased from 1.27×10^{-7} to $2.04\times10^{-8}\,g\,m^{-3}$ and 1.23×10^{-7} to $9.45\times10^{-9}\,g\,m^{-3}$ and the time to peak concentration increased from 10.2 to 81.6 h and 16.8 to 81.6 h, respectively (Figs. 3b and c). As moisture was increased, the peak concentration of toluene and *p*-xylene decreased to 1/6 and 1/12 and the time of peak concentration increased by a factor of 8 and 5, respectively (Figs. 3b and c).

These results indicate that the increased advection and the reduced pore space for available diffusive transport significantly reduced the peak indoor air concentration of VOC-odor in the ventilated airspace. Generally, volatilization increased during periods of low manure moisture and moisture advection, and decreased when moisture levels and moisture content increased. This illustrates the extreme sensitivity of predicted VOC-odor concentration to even small variations in manure moisture behavior. At the lower moisture content, the downward advection of moisture had little effect on the time course and magnitude of VOC-odor concentration. Under these conditions, diffusion transport was the dominant transport mechanism because of relatively large volume of air space available in the manure and the low moisture advection.

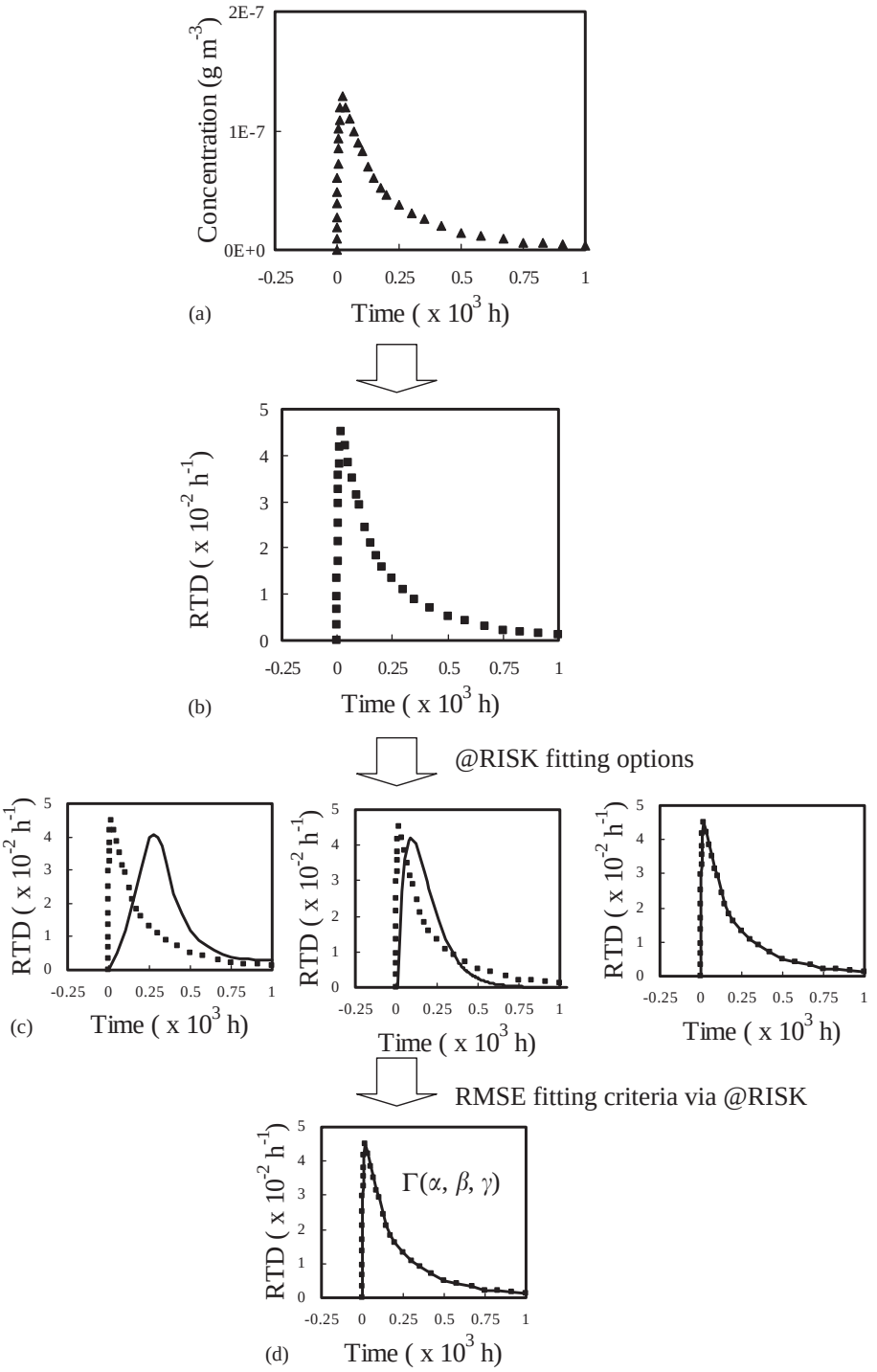

Fig. 2. Fitting process of MARGM: (a) schematic VOC-odor concentration versus time profile, (b) transforms to RTD, (c) chooses fitting parameters, and (d) finds out the best fitting parameters of three-parameter gamma distribution.

3.2. Curve-fitting by MARGM

Figs. 4–6 show the best-fitting probability density functions and their corresponding parameter values for *p*-cresol, toluene, and *p*-xylene, respectively. The distribution of VOC-odor concentration from θ of 60 to 80% in the swine housing is right skewed and the shape of the distribution of toluene or *p*-xylene is more peak

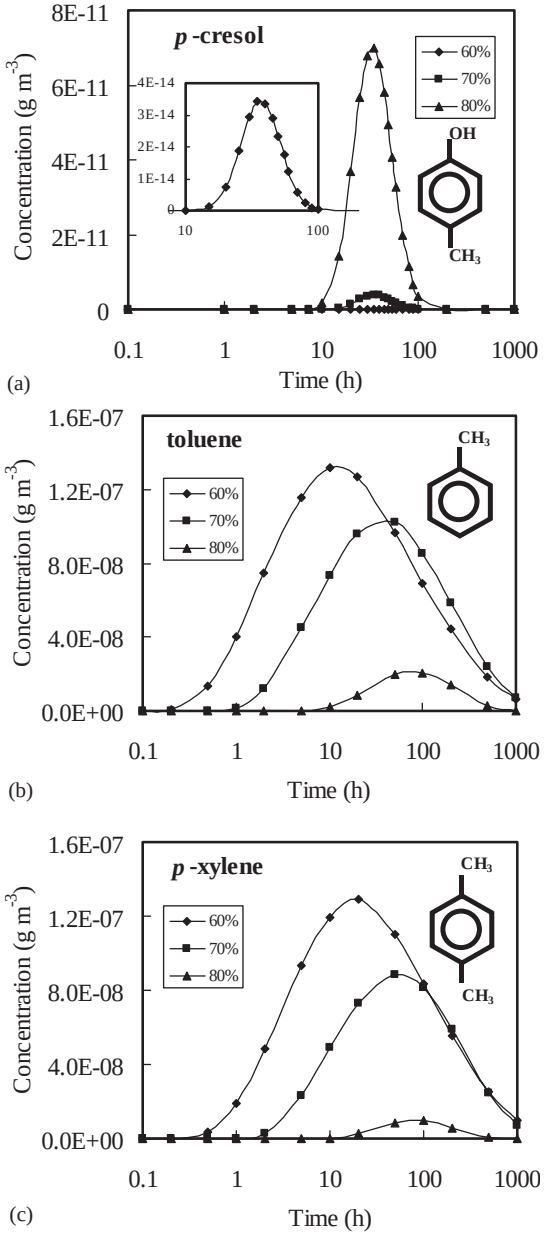

Fig. 3. Predicted concentration profiles of (a) *p*-cresol, (b) toluene, and (c) *p*-xylene by VOC-odor transport model under different moisture contents.

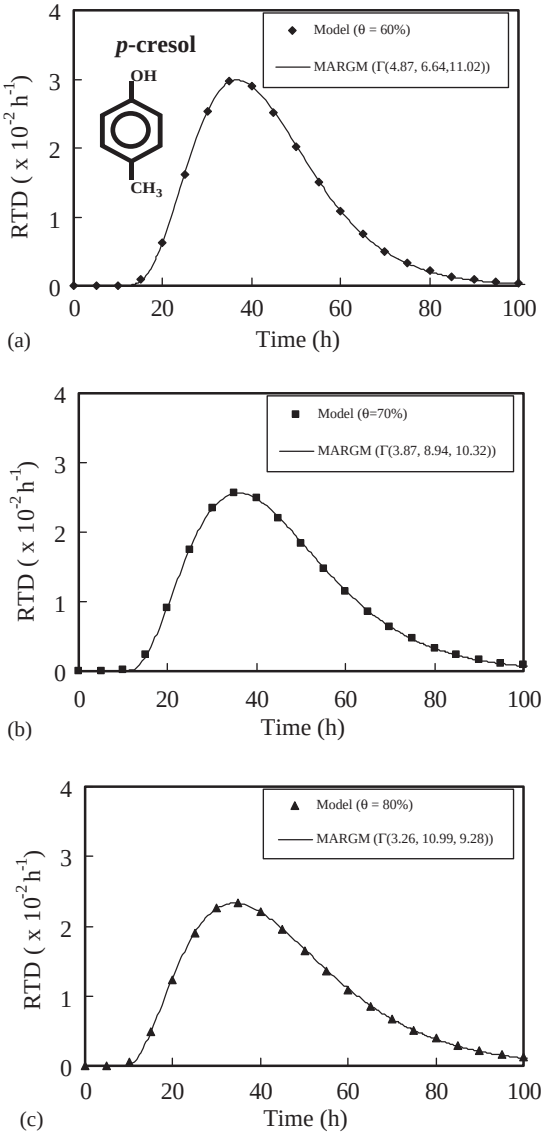

Fig. 4. *p*-cresol concentration profile predicted from transport model fitted by MARGM at different moisture contents: (a) $\theta = 60\%$, (b) $\theta = 70\%$, and (c) $\theta = 80\%$ ($Q = 0.05\,m^3\,s^{-1}\,pig^{-1}$).

than that of *p*-cresol. The $\Gamma(4.87, 6.64, 11.02)$ distribution showed the best fitting curve when θ of *p*-cresol was 60% (Fig. 4a). Under this fitting scenario, 5% of *p*-cresol would be exhausted before 23.59 h, 90% would be exhausted between 23.59 and 70.68 h, and only 5% exited over 70.68 h. The best fitting distribution at θ of 70 and 80% were determined as $\Gamma(3.87, 8.94, 10.32)$ and $\Gamma(3.26, 10.99, 9.28)$, respectively (Figs. 4b and c). The shape factor decreased from 4.87 to 3.26 when θ increased from 60 to 80% for *p*-cresol. On the contrary, the scale factor increased from 6.64 to 10.99 when θ increased.

The $\Gamma(1.03, 246.10, 1.80)$ distribution showed the best fitting curve when θ was 60% in that 5% of toluene would be exhausted before 15.63 h, and only 5% exited over 751.72 h (Fig. 5a). The $\Gamma(1.05, 330.43, 2.40)$ distribution showed the best fitting curve when θ was 60% in that 5% of *p*-xylene would be exhausted before 22.34 h, and only 5% exited over 1023.00 h (Fig. 6a).

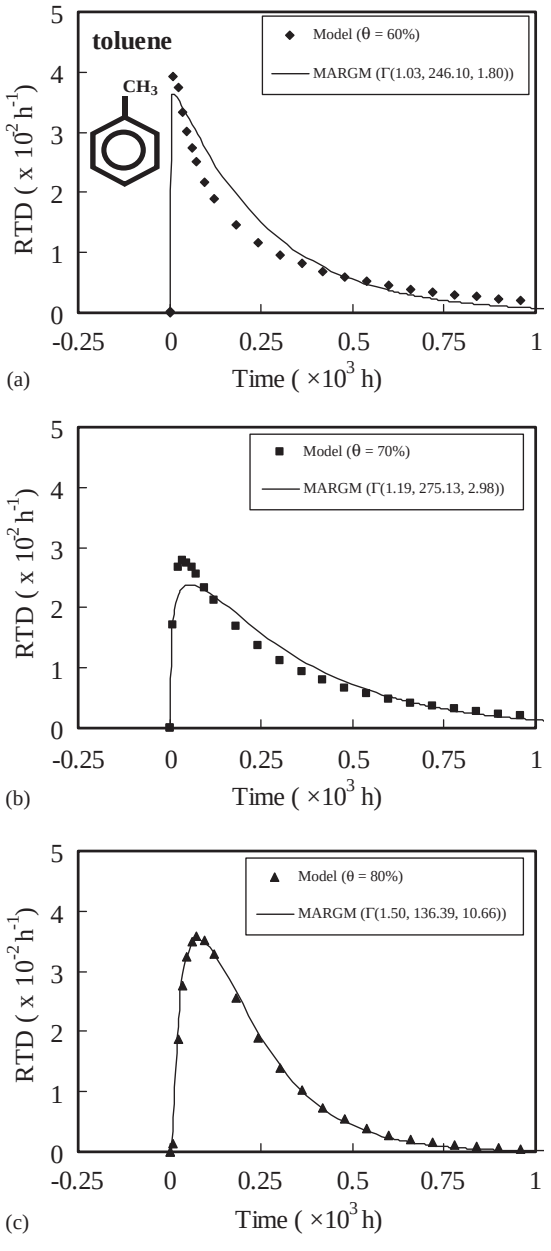

Fig. 5. Toluene concentration profile predicted from transport model fitted by MARGM at different moisture contents: (a) $\theta = 60\%$, (b) $\theta = 70\%$, and (c) $\theta = 80\%$ ($Q = 0.10\,m^3\,s^{-1}\,pig^{-1}$).

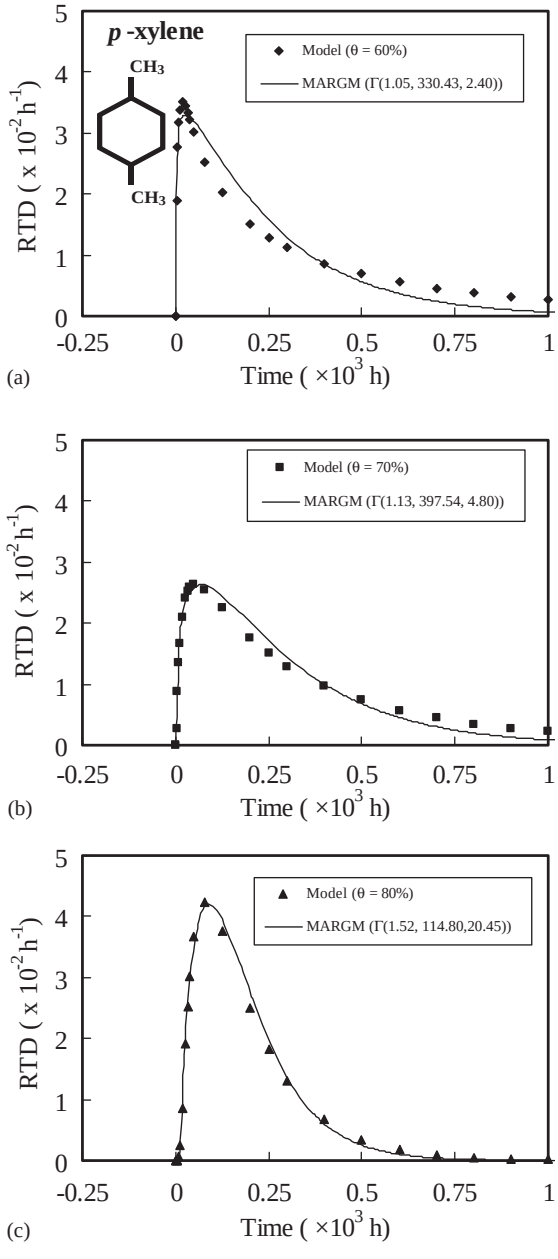

Fig. 6. *p*-xylene concentration profile predicted from transport model fitted by MARGM at different moisture contents: (a) $\theta = 60\%$, (b) $\theta = 70\%$, and (c) $\theta = 80\%$ ($Q = 0.075\,m^3\,s^{-1}\,pig^{-1}$).

When θ increased from 60 to 80%, the shape factors increased from 1.03 to 1.50 and 1.05 to 1.52 for toluene and *p*-xylene, respectively. The scale factor increased when θ increased from 60 to 70%, but decreased when θ increased from 70 to 80%.

95% of *p*-cresol exited swine housing before 4 days, and only 5% residue in the ventilated airspace for over 82.64 h at θ was 80%, while toluene and *p*-xylene showed the longer residence time stay in ventilated airspace than *p*-cresol did (Figs. 4–6). The concentration distribution period indicated that the influence of half-life for different chemicals. Due to the value of half-life is only 0.67 d for *p*-cresol, the concentration distribution period in the concentration profile of *p*-cresol significantly appeared between 10 to 100 h less than that of toluene with half-life of 22 d. The longer the half-life

was, the longer period of concentration distributed and the higher scale factor appeared in the distribution. The scale factor of either toluene or *p*-xylene was larger than that of *p*-cresol at the same θ as ventilation rate increased. The effect of half-life determined the major cause of concentration distribution period.

The concentration distribution had roughly similar shape for θ form 60 to 80% of the same chemicals. The *p*-cresol concentration distribution flattened out when θ increased. Since the environmental conditions were almost similar, the change in concentration distribution shape is most likely due to properties of chemical such as diffusion coefficient, etc.

3.3. Mean residence time and mixing factor estimates

Table 4 lists mean residence time and mean mixing factor calculated under different environmental conditions. The mean residence time of *p*-cresol at θ of 60% calculated by MARGM and VOC-odor concentration profile were 43.40 and 43.48 h, respectively. As θ increased, the mean residence time and mixing factor of *p*-cresol increased, yet insignificantly. The mean residence time calculated by MARGM and VOC-odor concentration profile of either toluene or *p*-xylene at θ of 60% showed significant difference with value of 140.61 and 106.49 h, respectively. It was due to the underestimate of concentration profile between 700 and 2500 h of either toluene or *p*-xylene at θ of 60%. The mean residence time difference between MARGM and VOC-odor concentration profile declined as θ increased. RMSE of three selected chemicals were all within 10^{-8}–10^{-9} order.

When ventilation rate (Q) was $0.05\,m^3\,s^{-1}\,pig^{-1}$, it could lead to approach the incomplete-mixing flow pattern. Since over 90% of mixing volume was constructed from incomplete mixing flow, the contributions from complete mixing and piston flow were insignificant and could be omitted. Mean mixing factor of *p*-cresol increased from 0.15 to 0.24 as θ increased from 60 to 80% due to the mixing factor in incomplete mixing volume increased from 0.16 to 0.25. As Q was increased from 0.05 to $0.075\,m^3\,s^{-1}\,pig^{-1}$, it could lead to approach the complete-incomplete mixing flow pattern. Mean mixing factor of *p*-xylene decreased from 0.95 to 0.59 as θ increased from 60 to 80% due to the mixing factor in incomplete mixing volume decreased from 0.92 to 0.52 and complete mixing volume decreased from 41.64 to 21.70%. When Q was increased to $0.10\,m^3\,s^{-1}\,pig^{-1}$, it also approached the incomplete-mixing flow pattern. Since over 90% of mixing volume was constructed from complete mixing and incomplete mixing flow, the contribution from piston flow was omitted. Mean mixing factor of toluene decreased from 0.96 to 0.63 as θ increased from 60 to 80% due to the mixing factor in incomplete mixing volume decreased from 0.95 to 0.51 and complete mixing volume decreased from 41.06 to 28.67%.

There was a large discrepancy of mean mixing factor between *p*-cresol and toluene, which was likely to have been caused by incomplete mixing of air within the building. Increase ventilation rate could lead to approach the complete-incomplete mixing flow pattern. Especially when θ was at 60% and the shape factor approached to 1, mean mixing factor was near 1 and the trend of complete mixing flow was evident in ventilation system. As moisture content increased and the shape factor may be over 1.5, resulting in a lowering the value of mean mixing factor.

Table 4
The mean residence time (T) and mean mixing factor ($\bar{\zeta}$) calculated by MARGM and VOC-odor concentration profile under different environmental conditions

Chemical	Q ($m^3s^{-1}pig^{-1}$)	θ (%)	T_{MARGM}[a] (h)	$T_{VOC-odor}$[b] (h)	RMSE (h^{-1})	ζ	V_i/V (%)	V_c/V (%)	V_p/V (%)	$\bar{\zeta}$[c]
p-cresol	0.05	60	43.40	43.48	1.50×10^{-8}	0.16	94.60	0.18	5.22	0.15
	0.05	70	44.89	44.90	2.06×10^{-8}	0.20	92.70	1.36	5.94	0.20
	0.05	80	45.06	44.94	2.68×10^{-8}	0.25	92.43	1.26	6.31	0.24
toluene	0.10	60	254.47	395.18	4.94×10^{-8}	0.95	58.25	41.06	0.69	0.96
	0.10	70	331.56	386.60	1.29×10^{-8}	0.72	59.52	39.73	0.75	0.83
	0.10	80	215.87	233.28	3.84×10^{-9}	0.51	68.03	28.67	3.30	0.63
p-xylene	0.075	60	348.83	455.32	2.65×10^{-8}	0.92	57.71	41.64	0.66	0.95
	0.075	70	453.21	404.18	2.04×10^{-8}	0.82	63.04	36.02	0.94	0.88
	0.075	80	195.11	198.83	1.52×10^{-9}	0.52	71.41	21.70	6.89	0.59

[a] Mean residence time calculated by MARGM.
[b] Mean residence time calculated by VOC-odor transport model (Jury et al., 1990).
[c] Mean mixing factor calculated by Eq. (19).

3.4. Effect of chemical properties and moisture content

The chemical property that is principally responsible for volatilization of VOC-odor from swine manure is the effective diffusion coefficient (D_E). For the VOC-odor that reside principally in the vapor phase this coefficient is essentially proportional to the 10/3 power of the volumetric air content if one considers the tortuosity as expressed in Eq. (3). For this reason, increasing the moisture content of the confining layer significantly decreases volatilization flux over any time period. However, it may be difficult to maintain moisture content of swine manure due to operation of swine ventilation systems and animal activities.

Properties of VOC-odor and moisture contents were major cause to affect VOC-odor concentration. Effective diffusion coefficient of toluene decreased as moisture content increases. On the contrary, D_E of *p*-cresol increases from 1.89×10^{-10} to $3.86 \times 10^{-10}\,m^2\,s^{-1}$ as θ increases from 60 to 80%, indicating the effect of low Henry's constant (K_H) of *p*-cresol to cause different results compare with toluene and *p*-xylene.

3.5. Physical meaning of gamma distribution parameters

The change of shape parameter in gamma distribution is most likely due to properties of chemical such as D_E, K_H, and half-life. The value of scale parameter was determined mostly by the effect of half-life, indicating different distribution period in concentration profile. Since toluene and *p*-xylene had half-life value with 22 and 28 d, respectively, indicating the longer concentration distributed period (Figs. 5–6) and the larger scale parameter than that of *p*-cresol (Fig. 4) did. The location parameter implies the time when VOC-odor was detected after emission from swine manure.

4. Conclusions

The incorporation of VOC-odor transport model into multiple airflow regions gamma model (MARGM) has the potential to estimate mean residence time and mixing factor in ventilation system characterized by different mixing regimes. The three-parameter gamma distribution was chosen due to its factorial property to reduce mathematical terms and the unique feature whereas the other end is distributed over a large scale of the variant. The mixing type of piston flow, incomplete mixing, and complete mixing can be obtained from various forms of RTD functions. The model goes into enough detail in that the meaningful physical phenomena are taken into account, whereas at the same time retains enough simplicity to minimize data input requirements. Heterogeneous mixing is simulating free from the disperse limitation which was scale dependent. The accuracy of MARGM is considered to be sufficient for preliminary feasibility studies. It is hoped that additional experimental data with well-documented test information can be used to confirm the overall applicability to model indoor air quality response to environmental disturbances.

Acknowledgements

The authors wish to acknowledge the financial support of the National Science Council of Republic of China under the grant NSC91-2313-B002-295.

References

Chang, C.W., Chung, H., Huang, C.F., Su, H.J.J., 2001. Exposure assessment to airborne endotoxin, dust, ammonia, hydrogen sulfide and carbon dioxide in open style swine houses. The Annals of Occupational Hygiene 45, 457–465.

Cheng, T.B., Jiang, Y., Xu, Y., Zhang, Y.P., 2002. Mathematical model for simulation of VOC emissions and concentrations in buildings. Atmospheric Environment 36, 5025–5030.

Chung, Y.C., Huang, C.P., Tseng, C.P., 1996. Reduction of H_2S/NH_3 production from pig feces by controlling environmental conditions. Journal of Environmental Science and Health A 31, 139–155.

Clanton, C.J., Schmidt, D.R., Nicolai, R.E., Jacobson, L.D., Goodrich, P.R., Janni, K.A., Bicudo, J.R., 2001. Geotextile fabric-straw manure storage covers for odor, hydrogen sulfide, and ammonia control. Applied Engineering in Agriculture 17, 849–858.

Donham, K.J., 2000. The concentration of swine production: effects on swine health, productivity, human health, and the environment. the veterinary clinics of North America. Food Animal Practice 16, 559–597.

Howard, P.H., Boethling, R.S., Jarvis, W.F., Meylan, W.M., Michalenko, E.M., 1991. Handbook of Environmental Degradation Rates, Lewis, Michigan. p. 366, 410, 643.

Huang, H.Y., Haghighat, F., 2002. Modeling of volatile organic compounds emission from dry building materials. Building and Environment 37, 1127–1138.

Jury, W.A., Russo, D., Streile, G., Abd, H.E., 1990. Evaluation of volatilization by organic chemicals residing below the soil surface. Water Resources Research 26, 13–20.

Karimipanah, T., Awbi, H.B., 2002. Theoretical and experimental investigation of impinging jet ventilation and comparison with wall displacement ventilation. Building and Environment 37, 1329–1342.

Levenspiel, O., 1999. Chemical Reaction Engineering. Wiley, New York, pp. 257–292.

Liang, H.M., 2002. Dynamic transport of livestock generated VOC-odor in a ventilated airspace with mixing heterogeneity. Unpublished Ph.D. Dissertation, National Taiwan University, Taipei, Taiwan.

Liao, C.M., Chen, J.W., Huang, M.Y., Chen, J.S., Chang, T.J., 2001. An inhalation dose model for assessing dust-borne

VOC-odor exposure from feeding in swine buildings. Transactions of the ASAE 44, 1813–1824.

Louhelainen, K., Kangas, J., Veijanen, A., Viilos, P., 2001. Effect of in situ composting on reducing offensive odors and volatile organic compounds in swineries. American Industrial Hygiene Association Journal 62, 159–167.

Schiffman, S.S., Bennett, J.L., Raymer, J.H., 2001. Quantification of odors and odorants from swine operations in North Carolina. Agricultural and Forest Meteorology 108, 213–240.

Thibodeaux, L.J., 1996. Environmental Chemodynamics. Wiley, New York, pp. 554–558.

Weber, W.J., DiGiano, F.A., 1995. Process Dynamics in Environmental Systems. Wiley, New York, pp. 321–422.

Wong, N.H., Mahdavi, A., Boonyakiat, J., Lam, K.P., 2003. Detailed multi-zone air flow analysis in the early building design phase. Building and Environment 38, 1–10.

Young, P., Price, L., Berckmans, D., Janssens, K., 2000. Recent revelopments in the modelling of imperfectly mixed airspaces. Computers and Electronics in Agriculture 26, 239–254.